CHEMISTRY
A EUROPEAN JOURNAL

DOI: 10.1002/chem.201003355

Carbon-Nanotube-Based Stimuli-Responsive Controlled-Release System

Xuecheng Chen,[a] Hongmin Chen,[b] Carla Tripisciano,[a] Anna Jedrzejewska,[a] Mark H. Rümmeli,[c] Rüdiger Klingeler,[c] Ryszard J. Kalenczuk,[a] Paul K. Chu,*[b] and Ewa Borowiak-Palen*[a]

Abstract: A stimuli-responsive controlled-release delivery system based on carbon nanotubes is demonstrated. Through TEM, FTIR spectroscopic, and thermogravimetric analysis, functional groups have been successfully attached to the open ends of the tubes, thereby enabling functionalized silica spheres to preferentially attach to the ends. This, in essence, plugs the ends of the tube. Controlling release of encapsulated materials within the tubes is illustrated by fluorescein-filled carbon nanotubes. The discharge process can be triggered by exposure to 1,4-dithiothreitol (DTT) or at elevated temperature. Moreover, both triggering systems, DTT and temperature, provide rate of release control through increased DTT concentration or temperature choice, respectively. This delivery system paves the way for the development of a new generation of site-selective, controlled-release, drug-delivery systems, and interactive nanosensor devices.

Keywords: carbon · drug delivery · fluorescein · nanotubes · stimuli response

Introduction

There is tremendous interest in the use of nanomaterials to deliver biologically active cargo such as drugs and DNA to specific sites in living systems for disease diagnosis and therapeutic treatment.[1] Among the potential candidates, carbon nanotubes (CNTs) rank highly due to their unique physical, chemical, and physiological properties. CNTs have very interesting physicochemical properties such as ordered structure with high aspect ratio, ultralight weight, high mechanical strength, high electrical conductivity, high thermal conductivity, and high surface area. The combination of these characteristics makes CNTs a unique material with the potential for diverse applications, including biomedical.[2] There is an increasing interest in exploring all of these properties that CNTs possess for applications that range from sensors for the detection of genetic or other molecular abnormalities, to substrates for the growth of cells for tissue regeneration. CNTs have also been proposed and actively explored as multipurpose innovative carriers for drug delivery and diagnostic applications. Their versatile physicochemical features enable the covalent and noncovalent introduction of several pharmaceutically relevant entities and allow for the rational design of novel candidate nanoscale constructs for drug development. CNTs can be functionalized with different functional groups to carry simultaneously several moieties for targeting, imaging, and therapy.[3] Very recently, carbon nanotubes have been shown to cross cell membranes easily and to deliver peptides, proteins, and nucleic acids into cells.[4] These innovative carriers present a lower toxicity, a fact that boosts their potential for biomedical applications.[5] Moderate biological effects have been achieved in these studies, but more importantly, they have proven the principle that CNTs can offer advantages in terms of their pharmacological utilization.

Clinical applications of CNTs also offer a great number of opportunities provided we are able to take advantage of the characteristics nanotubes offer. To date, two in vivo studies have demonstrated the potential of CNTs to help improve the characteristics of known therapeutics.[2a] In addition, the intrinsic stability and structural flexibility of CNTs may prolong the circulation time.[6] However, the release of an encapsulated cargo in many current delivery systems is dispersed immediately upon exposure to a water-based environment.[7] Hence, a controlled-release system to deliver the cargo is highly needed. In the last few years, several controlled-release systems have been developed. For example, CdS and Fe_3O_4 nanoparticles have been used as the capping agent to control the opening/closing of the pore entrance of

[a] Dr. X. Chen,[+] Dr. C. Tripisciano, Dr. A. Jedrzejewska, Prof. R. J. Kalenczuk, Prof. E. Borowiak-Palen
Institute of Chemical and Environment Engineering
West Pomeranian University of Technology
ul. Pulaskiego 10, 70-322 Szczecin (Poland)
E-mail: eborowiak@zut.edu.pl

[b] Dr. H. Chen,[+] Prof. P. K. Chu
Department of Physics and Materials Science
City University of Hong Kong
Tat Chee Avenue, Kowloon, Hong Kong (P. R. China)
E-mail: paul.chu@cityu.edu.hk

[c] Dr. M. H. Rümmeli, Prof. R. Klingeler
Leibniz Institute for Solid-State
and Materials Research Dresden
Helmholtzstrasse 20, 01069 Dresden (Germany)

[+] These authors contributed equally to this work.

Supporting information for this article is available on the WWW under http://dx.doi.org/10.1002/chem.201003355.

mesostructured materials.[8] A photo-controlled release system based on coumarin-functionalized mesoporous materials has also been demonstrated.[9] Polyamines anchored on the pore outlets of mesoporous materials that serve as a dual pH- and anion-driven gatelike ensemble have also been shown.[10] A series of supermolecular nanovalves that use redox,[11] pH,[12] competitive binding,[11,13] light,[12,14] and enzymes[15] as actuators constitutes another approach.

In this article, to advance the field of CNTs and as proof-of-concept, we present an attractive, controllable gatelike approach in which silica nanospheres seal the tips of open-ended multiwalled carbon nanotubes that have been filled with dye guest molecules (fluorescein). The CNTs can be re-opened by removing the silica spheres by means of different external stimuli.

Results and Discussion

The efficiency of the developed methodology was assessed by encapsulating and sealing fluorescein molecules in the carbon nanotubes (CNTs). The encapsulated fluorescein was released from the tubes in a controlled manner by cleaving the chemical bond between the silica nanosphere and CNT. This can be achieved by the addition of disulfide reducing agents (e.g., dithiothreitol (DTT)) or thermal treatment. The preparation process for the sealed filled CNT is depicted in Scheme 1. Initially, the CNTs are opened using a

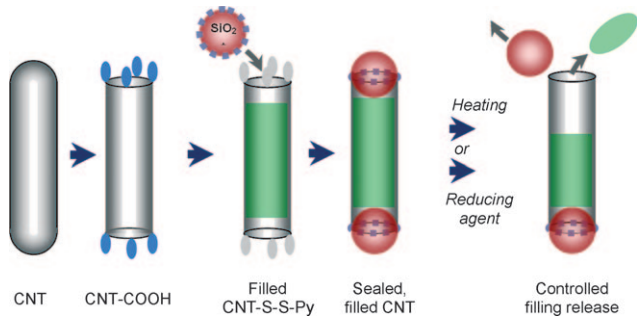

Scheme 1. Schematic of the synthesis steps for a stimuli-responsive system based on carbon nanotubes capped with functionalized silica nanospheres and their controlled release.

heat/oxidation process, which forms carboxyl groups at the open ends of the tubes (CNT-COOH). In the next step, *S*-(2-aminoethylthio)-2-thiopyridine reacts with the CNT-COOH to form thiopyridine-functionalized CNT ends (CNT-S-S-Py). The filling (fluorescein) is then placed into the cores of the tubes, and then the nanotubes are sealed by the addition of thiol-silica nanospheres (Figure S3 in the Supporting Information). The spheres selectively conjugate to the CNT ends by means of a thiol coupling reaction (CNT-S-S-SiO_2), essentially a capping mechanism. The sealed CNTs can be reopened by cleaving the disulfide bond (-S–S-) and exposure to disulfide reducing agents (e.g., DTT). Alternatively, they can be reopened by heating. Once opened, the contents are released. In other words, controlled cap ejection governs the release of the contents within the CNTs.

Figure 1 shows the FTIR spectra of CNT-COOH (spectrum A), CNT-S-S-Py (spectrum B), and CNT-S-S-SiO_2 (spectrum C). In the FTIR spectrum of multiwalled carbon

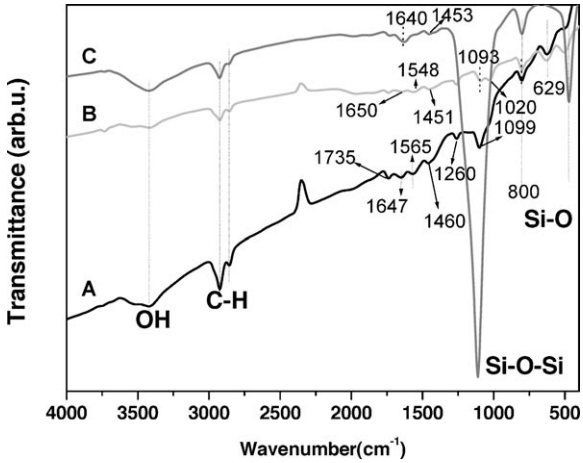

Figure 1. FTIR spectra of A) carboxylic acid-modified CNTs (CNT-COOH), B) CNTs with thiol functionality (CNT-S-S-Py, C) and the silica sphere conjugates with CNTs (CNT-S-S-SiO_2).

nanotube (CNT)-COOH, the characteristic peak of the –COOH functionality at 1735 and 3417 cm^{-1} are present. The band at 1460 cm^{-1} is attributed to the C=O stretching mode quinone group. The peaks at 800 and 1260 cm^{-1} correspond to C–O (from the ester), which is attached to the aromatic group. The peak at 1099 cm^{-1} is related to sulfate groups, and the bands at 2855 and 2923 cm^{-1} arise from the stretching vibrations of -CH_2- bonds. The peaks at 1647 and 1565 cm^{-1} are ascribed to the carbon skeleton.[16] In the fingerprint region, the peak seen at 620 cm^{-1} can indicate a bending vibration of CH bonding. These peaks verify that the CNTs have been successfully functionalized with carboxylic acid groups (–COOH). *S*-(2-Aminoethylthio)-2-thiopyridine was then treated with CNT-COOH (catalyzed by ethylene dichloride (EDC)) to form CNT-S-S-Py, as shown in Scheme 1. In the FTIR spectrum of CNT-S-S-Py, the characteristic peak of acylamide at 1650 cm^{-1} intensifies, and the new characteristic peaks at 1451, 1548, and the newly appeared peak at 1020 cm^{-1} associated with pyridine rings are visible. This indicates that the amidation reaction of $-NH_2$ (S-(2-aminoethylthio)-2-thiopyridine) with –COOH (CNT) group has occurred, and that thiol-reactive functionalities are anchored onto the CNTs (Figure S2 in the Supporting Information). Other peaks of CNT-S-S-Py are almost same as CNT-COOH. In the FTIR spectrum of fluorescein-filled CNT-S-S-SiO_2, new strong peaks at around 1100, 800, and 474 cm^{-1} appeared, which correspond to the Si-O-Si bond; these peaks come from thiol-group-functionalized silica spheres. This confirms that the silica spheres are chemically

bound to the CNTs. The graph of the second derivative of FTIR transmittance spectra of the samples is also shown in Figure S11 in the Supporting Information.

Figure 2A displays a TEM image of a CNT after the purification/opening treatment. Here one can see that CNT has been opened upon heat treatment in air at 400 °C. Systematic microscopic analysis of the sample proved the successful opening of the tubes in the bulk sample. This was also confirmed by BET specific area measurements of raw and purified/opened CNT, which increased from 117 to 143 $m^2 g^{-1}$, respectively. The outer diameter of the CNTs ranges between 9 and 25 nm (mean diameter of 15 nm). The length of the oxidized CNT is smaller than 500 nm. Figure 2B shows a TEM image of a CNT with encapsulated fluorescein (as indicated by arrows); if there is no fluorescein, the inside of the CNT should be clear. Similar TEM images are also shown in Figure S3 in the Supporting Information. In the CNT, black dots have been detected. They could be attributed to the presence of fluorescein. These data show that fluorescein has been successfully stored in the CNT. The functionalized silica nanospheres (SiO_2–SH), as depicted in Figure 1C, have a diameter range between 5 and 30 nm (mean diameter 15 nm). The FTIR spectra of SiO_2 and SiO_2–SH are depicted in Figure S4 in the Supporting Information; these demonstrate that thiol groups have been successfully functionalized on the surface of silica spheres. TEM studies of the tubes after the sealing process show a variety of sealed tubes in which a single sphere seals a tube end (Figure 2D and E) or in which a cluster of 2–4 spheres seals a tube as, for example, shown in Figure 2F and Figure S5 in the Supporting Information in detail (CNT-S-S-SiO_2). It is important to point out that the surface of the CNT is very clear, thus indicating that fluorescein is stored in the inner space of CNT but not on the surface (Figure S5).

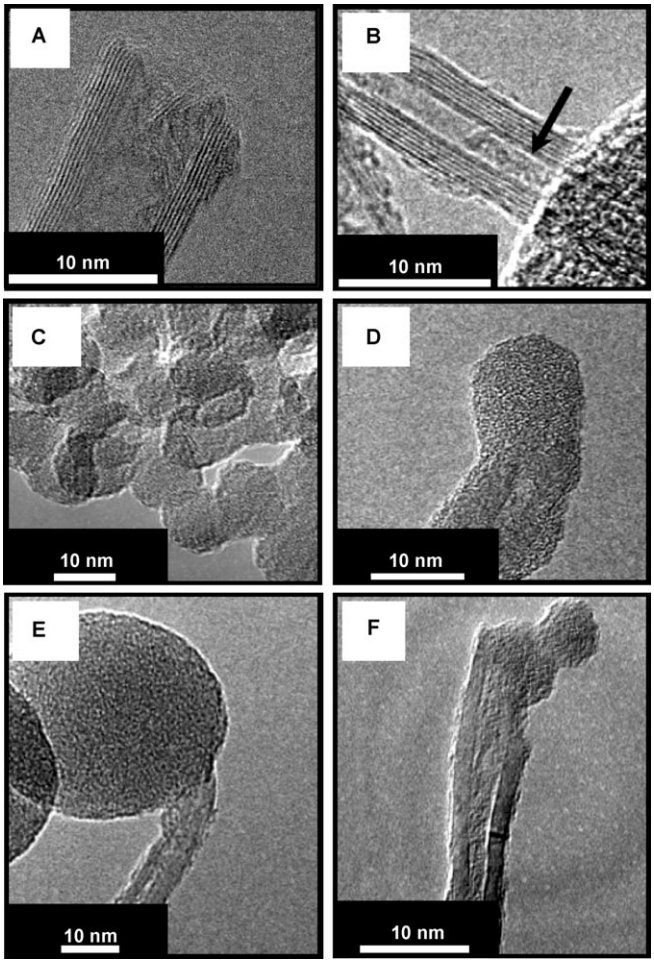

Figure 2. TEM images of A) open-ended CNT, B) CNT encapsulating fluorescein, C) thiol-silica nanospheres, D) CNT capped with a silica sphere, E) CNT capped with a large silica sphere, and F) CNT capped with a small cluster of silica spheres.

The Raman spectra of fluorescein and the fluorescein@CNT-S-S-SiO_2 excited at 514 nm are shown in Figure 3. One can clearly see that the peaks corresponding to graphitic CNTs (D mode $\approx$1340 cm^{-1}, G mode $\approx$1570 cm^{-1}, and 2D mode $\approx$2670 cm^{-1}) dominate the Raman response. However, the weak peaks ascribed to fluorescein encapsulated in the carbon nanotube at 1196, 1337, 1461, 1533, 1612, 1651 cm^{-1} are still detectable. Additionally, the BET total specific surface value calculated from the N_2 adsorption–desorption of the samples was measured. Here, the BET specific surface value of the oxidized CNTs (open state) was 143.63 $m^2 g^{-1}$. After encapsulation with fluorescein and capping with silica spheres, the BET specific surface value dropped to 83.37 $m^2 g^{-1}$, thereby indicating that significant pore blocking has occurred. It is worth noting that the BET area of the synthesized silica spheres was 200 $m^2 g^{-1}$. Therefore, both TEM and N_2 adsorption–desorption confirm the successful opening of the carbon nanotubes as well as their being filled and their ends being sealed or capped.

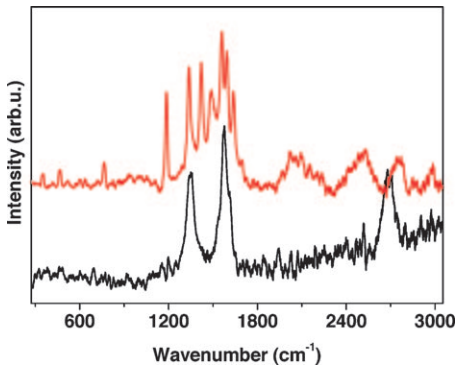

Figure 3. Raman spectra of fluorescein (in red) and fluorescein encapsulated in the channel of CNT (fluoresecin@CNT-S-S-SiO_2; in black).

Thermogravimetric analysis (TGA) measurements from purified CNT, fluorescein, and fluorescein stored in CNTs (fluoresecein@CNT) are presented in Figure 4. As shown in

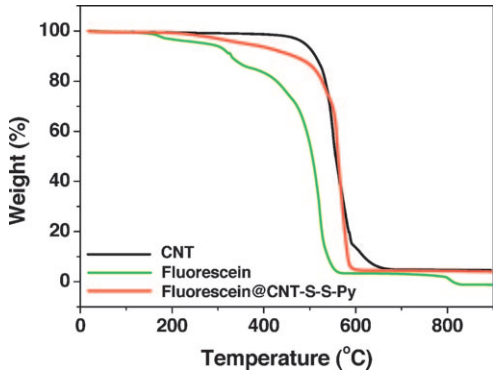

Figure 4. TGA graphs of fluorescein (in green), purified CNTs (in black), and fluorescein@CNT-S-S-Py (in red).

Figure 4, fluorescein begins to decompose at 160 °C in air, and above 557 °C it is almost completely decomposed (green line). However, purified CNTs begin to decompose at 585 °C in air, and when the temperature is further increased, weight loss increases rapidly until all the CNTs are exhausted at about 700 °C (black line). The sample of fluoresecein@CNT-S-S-Py exhibits TGA behavior similar to that of the purified CNT under these experimental conditions. The only difference is the temperature of starting decomposition. Fluoresecein@CNT-S-S-Py begins to decompose at 240 °C, which comes from fluorescein. The temperature is little higher than fluorescein and this is because of the protection from CNT. For all of three samples, the change in TGA residues at 900 °C is around 3.6 % (w/w), which may come from iron oxide trapped in the CNT. The amount of fluorescein loaded in the CNTs was estimated by TGA studies according to the difference in the weight loss in Figure 4. The data reveal a loading of around 40 wt % fluorescein in the CNTs. Based on the above TGA data, for the sample of fluoresecein@CNT-S-S-Py, fluorescein is indeed trapped in the channels of CNT and not on the surface of the CNT, which is consistent with TEM and BET results.

To investigate the effectiveness of the stimuli-responsive release mechanism, UV/Vis absorption spectroscopy was employed. In essence, the intensity fluorescein absorption band at 491 nm (Figure 5A) was monitored with respect to time. The sealed, fluorescein-filled CNTs were dispersed in the phosphate buffered saline (PBS) solution, and in the first study, 1×10^{-2} M DTT was added to the buffered, sealed, filled CNTs at room temperature. Before adding the DTT, no signal could be observed, but upon addition of the DTT, the signal rose relatively rapidly over the first few minutes, after which the signal stabilized. This clearly shows that the release of the fluorescein dye is triggered by DTT. A further study investigated the dependence of the DTT concentration after exposure for 24 h; the results at room temperature are presented in Figure S6 in the Supporting Information and Figure 5C. The data imply that the stable release level of the dye increases at higher DDT concentrations. The release level is probably related to the rate of release of the silica spheres off the tube ends. Our data show that the DTT concentration can be used to tailor the release of encapsulated molecules.

We have also investigated the role of temperature. Four temperatures were studied: room temperature (299 K), 313, 333, and 353 K (Figure 5D, Figure S7 in the Supporting Information). The data show no release at room temperature (similar to the previous study). However, a linear increase appears in the fluorescein dye signal with increasing temperature, thereby confirming that elevated temperature triggers the release of encapsulated materials and the rate depends on the chosen temperature. With regard to DTT-triggered release, the buffered solution turned green after release, thereby providing visual evidence of the fluorescein dye being discharged from the CNT (see Figure 5, right panels). Most likely, the release of the functionalized silica spheres from the CNTs tips occurs through the thermally stimulated cleavage of the amide bonds (-NH–CO-). In the case of DTT triggering the discharge, cleavage of the -S–S- bonds is probable. We have also conducted TEM measurements of the sample after DTT (1×10^{-2} M) and temperature-dependant (80 °C) release. The TEM images confirm that most of silica spheres have been successfully removed from the ends of CNTs after the release experiments. However, some fluorescein adsorbs onto the outer surface of CNTs or is still encapsulated in the inner space of CNTs due to the interaction between fluorescein and CNTs (Figures S8 and S9 in the Supporting Information). We propose a model for fluorescein release from CNTs after silica-sphere removal. After the fluorescein molecules are released from the tube, some of them go into the solution (this is why the solution be-

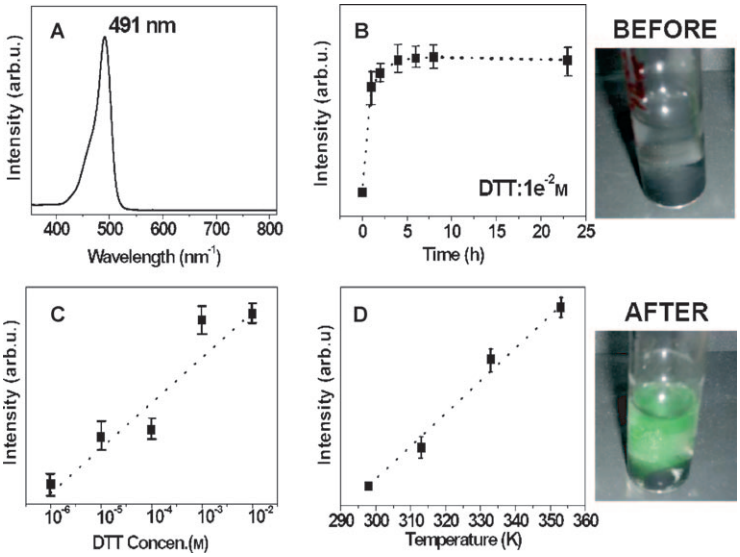

Figure 5. A) The typical UV/Vis absorption spectrum from fluorescein. B) Fluorescein release with respect to time from filled and capped CNTs in the presence of DTT at room temperature (DTT concentration: 1×10^{-2} M). C) UV/Vis spectra of DTT-concentration-dependent release at room temperature. The concentrations were measured after 24 h. D) UV/Vis spectra of temperature-dependent release (5.0 mg of the sample dispersed in 10.0 mL of PBS solution (pH 7.4)). The right panel images show typical examples of the buffered CNTs before triggering release (upper) and after release (lower).

comes green). In addition, some of the fluorescein adsorbs to the outer surface of the CNTs (Figure S10 in the Supporting Information).

Conclusion

We have demonstrated a novel route to produce filled CNTs and controlled discharge of the filling molecules, namely, a stimuli-responsive delivery system. The loading and release mechanism of the CNTs is based on the capping and uncapping of the open CNT ends with silica nanospheres. The discharge process can be triggered by exposure to DTT or at elevated temperature. Moreover, both triggering systems, DTT and temperature, provide rate of release control through increased DTT concentration or temperature choice, respectively. Both triggering systems work by cleaving the bond on the functional groups that attach the silica spheres to the open ends of the CNT. This delivery system paves the way for the development of a new generation of site-selective, controlled-release, drug-delivery systems, and interactive nanosensor devices. Future investigation will focus on the potential of the delivery systems for anticancer drugs.

Experimental Section

Materials: 3-Mercaptopropyltrimethoxysilane (MPTMS), tetraethyl orthosilicate (TEOS), acetic acid, methanol, dithiothreitol (DTT), L-lysine, fluorescein, 3-aminopropyltrimethoxysilane (APTS), 2-aminoethanethiol hydrochloride, 1-[3-(dimethylamino)propyl]-3-ethylcarbodiimide hydrochloride (EDC), aldrithiol-2, and octane were purchased from Aldrich and used as received.

Synthesis of raw multiwalled carbon nanotubes (CNTs): The CNTs were synthesized by using a chemical vapor deposition (CVD) technique described in details elsewhere.[17] A TEM image of the raw carbon nanotubes (before oxidation) is presented in Figure S1 in the Supporting Information.

Synthesis of carboxylic acids at the end of carbon nanotubes (CNT-COOH): The raw CNTs were first heated in air at 400 °C for 3 h to open the CNTs, and the treated CNTs were oxidized in a 4:1 mixture of concentrated H_2SO_4/H_2O_2 (30% aqueous) and stirring at 70 °C for 24 h to produce oxygen-containing groups at both ends, of which some were carboxylic acids. Then, CNT-COOH was separated by several filtration and washing steps, and the solid obtained was dried for 48 h at 100 °C.

Synthesis of thiol-silica nanospheres: The silica nanospheres were synthesized according to the method reported.[18] A certain amount of MPTMS (1/10 of TEOS volume) was added to the above solution of silica spheres. After stirring for a further 8 h, the silica nanospheres were centrifuged and dried to obtain thiol-silica-functionalized nanospheres.

Synthesis of *S*-(2-aminoethylthio)-2-thiopyridine hydrochloride: Thiopyridyl disulfide (Aldrithiol-2, 4.42 g, 20 mmol) was dissolved in methanol (20 mL) and acetic acid (0.6 mL). 2-Aminoethylthiol hydrochloride (1.14 g, 10.0 mmol) in methanol (9 mL) was added drop by drop to this solution over a period of 30 min. The mixture was stirred for an additional 48 h and then evaporated under high vacuum to obtain a yellow oil. The product was washed with diethyl ether (50 mL) and dissolved in methanol (10 mL), precipitated by addition of cold anhydrous diethyl ether (300 mL), and collected by vacuum filtration.

Synthesis of CNTs with thiol functionality: CNT-COOH (100 mg) was dispersed in phosphate buffered saline (PBS) solution (30 mL, pH 7.4) and sonicated for 30 min. 1-[3-(Dimethylamino)propyl]-3-ethylcarbodiimide hydrochloride (EDC) (1.725 g, 9.0 mmol) and *S*-(2-aminoethylthio)-2-thiopyridine hydrochloride (2.0 g, 9.0 mmol) were added to the CNT-COOH in PBS. The mixture was allowed to stir for 36 h followed by filtration. The resulting functionalized CNTs were isolated and dried under vacuum at 40 °C.

Loading of fluorescein into the CNTs and conjugation of silica nanospheres onto CNTs by a thiol coupling reaction: The end-functionalized CNTs (10 mg) were stirred vigorously in a concentrated solution of fluorescein in the PBS solution (10.0 mL, 100.0 mM, pH 7.4) for 24 h, and then the purified thiol-silica nanospheres (5 mg) were added to the above suspension. The mixture was stirred for 24 h at room temperature, followed by filtration and many washing cycles with acetone and ethanol to remove unloaded fluorescein molecules and unreacted thiol-silica spheres. The filled and sealed CNTs were isolated and dried under vacuum for 10 h.

Characterization: The morphology and chemical composition of the samples were studied by high-resolution transmission electron microscopy (HRTEM, Tecnai F30 from FEI). The specimens for the microscopic studies were prepared on standard TEM copper grids. Resonance Raman measurements were conducted using a Renishaw InVia Raman Microscope spectrometer (excitation laser wavelength = 514 nm). UV/Vis adsorption spectra were recorded at room temperature using an IR Nicole 6700 ThermoScientific UV/Vis spectrophotometer. Thermogravimetric analysis was performed using a DTA-Q600 SDT thermogravimetric analyzer (air flow, heating ramp 5 °C min^{-1}; TA Instruments).

Acknowledgements

The work was supported by the European Community through the Marie Curie Research Training Network CARBIO under contract MRTN-CT-2006-035616, the Polish Foundation for Science (focus program F4/2010), and the City University of Hong Kong Strategic Research Grant (SRG) 7008009.

[1] a) C.-Y. Lai, B. G. Trewyn, D. M. Jeftinija, K. Jeftinija, S. Xu, S. Jeftinija, V. S. Y. Lin, *J. Am. Chem. Soc.* **2003**, *125*, 4451–4459; b) Q. Fu, G. V. R. Rao, L. K. Ista, Y. Wu, B. P. Andrzejewski, L. A. Sklar, T. L. Ward, G. P. Lopez, *Adv. Mater.* **2003**, *15*, 1262–1266.

[2] a) L. Lacerda, A. Bianco, M. Prato, K. Kostarelos, *Adv. Drug Delivery Rev.* **2006**, *58*, 1460–1470; b) H. Dai, *Surf. Sci.* **2002**, *500*, 218–241; c) R. Klingeler S. Hampel, B. Büchner, *Int. J. Hyperthermia* **2008**, *24*, 496–515.

[3] M. Prato, K. Kostarelos, *Acc. Chem. Res.* **2008**, *41*, 60–68.

[4] a) D. Pantarotto, C. D. Partidos, R. Graff, J. Hoebeke, J. P. Briand, M. Prato, *J. Am. Chem. Soc.* **2003**, *125*, 6160–6164; b) N. W. Shi Kam, T. C. Jessop, P. A. Wender, H. Dai, *J. Am. Chem. Soc.* **2004**, *126*, 6850–6851; c) N. W. Shi Kam, H. Dai, *J. Am. Chem. Soc.* **2005**, *127*, 6021–6026; d) D. Pantarotto, R. Singh, D. McCarthy, M. Erhardt, J. P. Briand, M. Prato, K. Kostarelos, A. Bianco, *Angew. Chem.* **2004**, *116*, 5354–5358; *Angew. Chem. Int. Ed.* **2004**, *43*, 5242–5246; e) Q. Li, J. M. Moore, G. Huang, A. S. Mount, A. M. Rao, L. L. Larcom, P. C. Ke, *Nano Lett.* **2004**, *4*, 2473–2477.

[5] a) A. Bianco, K. Kostarelos, C. D. Partidos, M. Prato, *Chem. Commun.* **2005**, 571–577; b) K. Kostarelos, L. Lacerda, C. D. Partidos, M. Prato, A. J. Bianco, *J. Drug Delivery Sci. Technol.* **2005**, *15*, 41–47; c) V. L. Colvin, *Nat. Biotechnol.* **2003**, *21*, 1166–1170.

[6] Z. Liu, W. Cai, L. He, N. Nakayama, K. Chen, X. Sun, X. Chen, H. Dai, *Nat. Nanotechnol.* **2006**, *2*, 47–52.

[7] a) S. Radin, P. Ducheyne, T. Kamplain, B. H. Tan, *J. Biomed. Mater. Res.* **2001**, *57*, 313–320; b) W. Aughenbaugh, S. Radin, P. Ducheyne, *J. Biomed. Mater. Res.* **2001**, *57*, 321–326.

[8] S. Giri, B. G. Trewyn, M. P. Stellmaker, V. S.-Y. Lin, *Angew. Chem.* **2005**, *117*, 5166–5172; *Angew. Chem. Int. Ed.* **2005**, *44*, 5038–5044.

[9] a) N. K. Mal, M. Fujiwara, Y. Tanaka, *Nature* **2003**, *421*, 350–353; b) N. K. Mal, M. Fujiwara, Y. Tanaka, T. Taguchi, M. Matsukata, *Chem. Mater.* **2003**, *15*, 3385–3394.

[10] R. Casasus, E. Climent, M. D. Marcos, R. Martinez-Manez, F. Sancenon, J. Soto, P. Amoros, J. Cano, E. Ruiz, *J. Am. Chem. Soc.* **2008**, *130*, 1903–1917.

[11] a) T. D. Nguyen, H.-R. Tseng, P. C. Celestre, A. H. Flood, Y. Liu, J. F. Stoddart, J. I. Zink, *Proc. Natl. Acad. Sci. USA* **2005**, *102*, 10029–10034; b) T. D. Nguyen, Y. Liu, S. Saha, K. C.-F. Leung, J. F. Stoddart, J. I. Zink, *J. Am. Chem. Soc.* **2007**, *129*, 626–634.

[12] S. Angelos, Y.-W. Yang, K. Patel, J. F. Stoddart, J. I. Zink, *Angew. Chem.* **2008**, *120*, 2254–2258; *Angew. Chem. Int. Ed.* **2008**, *47*, 2222–2226.

[13] K. C.-F. Leung, T. D. Nguyen, J. F. Stoddart, J. I. Zink, *Chem. Mater.* **2006**, *18*, 5919–5928.

[14] T. D. K. Nguyen, C. F. Leung, M. Liong, Y. Liu, J. F. Stoddart, J. I. Zink, *Adv. Funct. Mater.* **2007**, *17*, 2101–2110.

[15] K. Patel, S. Angelos, W. R. Dichtel, A. Coskun, Y.-W. Yang, J. I. Zink, J. F. Stoddart, *J. Am. Chem. Soc.* **2008**, *130*, 2382–2383.

[16] a) A. Eitan, K. Y. Jiang, D. Dukes, R. Andrew, L. S. Schadler, *Chem. Mater.* **2003**, *15*, 3198–3201; b) A. G. Osorio, L. Silveira, V. L. Bueno, C. P. Bergmann, *Appl. Surf. Sci.* **2008**, *255*, 2485–2489; c) S. X. Yang, X. Li, W. P. Zhu, J. B. Wang, C. Descorme, *Carbon* **2008**, *46*, 445–452.

[17] E. Borowiak-Palen, A, Bachmatiuk, M. Rümmeli, S. Costa, R. Kalenczuk, *Physica E* **2008**, *40*, 2227–2230.

[18] T. Yokoi, Y. Sakamoto, O. Terasaki, Y. Kubota, T. Okubo, T. Tatsumi, *J. Am. Chem. Soc.* **2006**, *128*, 13664–13665.

Received: November 22, 2010
Published online: March 22, 2011

